arXiv:1512.08359v1 [physics.class-ph] 28 Dec 2015

,

A discussion of Bl conservation on a two dimensional magnetic field plane in watt balances

Shisong Li,* Wei Zhao, and Songling Huang

(Dated: December 29, 2015)

The watt balance is an experiment being pursued in national metrology institutes for precision determination of the Planck constant h. In watt balances, the $1/r$ magnetic field, expected to generate a geometrical factor Bl independent to any coil horizontal displacement, can be created by a strict two dimensional, symmetric (horizontal r and vertical z) construction of the magnet system. In this paper, we present an analytical understanding of magnetic field distribution when the r symmetry of the magnet is broken and the establishment of the Bl conservation is shown. By using either Gauss's law on magnetism with monopoles or conformal transformations, we extend the Bl conservation to arbitrary two dimensional magnetic planes where the vertical magnetic field component equals zero. The generalized Bl conservation allows a relaxed physical alignment criteria for watt balance magnet systems.

I. INTRODUCTION

A handful of national metrology institutes (NMIs) have designed and constructed watt balances[1–7], a high-precision force comparator leading the effort in redefining the SI unit of mass, the kilogram (kg), in terms of the Planck constant h, expected to culminate in 2018[8]. A watt balance experiment is comprised of two modes of operation, i.e., weighing mode and velocity mode. In the weighing mode, the downwards gravitational force exerted on a test mass is compensated by an upward electromagnetic force generated by a current-carrying coil in a magnetic field. The electromagnet's geometrical factor $(Bl)_w$ is measured as

$$(Bl)_w = \frac{mg}{I}, \tag{1}$$

where m denotes the test mass, g the local gravitational acceleration, B the magnetic flux density at the coil position, l the coil wire length, and I the current through the coil. In the velocity mode, the coil is moved in the magnetic field at a constant, vertical velocity v, yielding an induced voltage U, and the geometrical factor $(Bl)_v$ is calibrated as

$$(Bl)_v = \frac{U}{v}. \tag{2}$$

By comparing the measured values of I and U to electrical quantum standards, i.e., the Josephson voltage standard[9] and the quantum hall resistance standard[10], the Planck constant h is determined by a ratio of mechanical power and electrical power, i.e.,

$$h = h_{90}\frac{(Bl)_w}{(Bl)_v} = h_{90}\frac{mgv}{UI}, \tag{3}$$

where $h_{90} \equiv 6.626068854... \times 10^{-34}$Js is a derived value of the Planck constant by the 1990 conventional electrical units[11]. In order for each watt balance to qualify for the redefinition of the kilogram in 2018, each instrument must accurately measure h with a relative uncertainty of several parts in 10^8.

In a good measurement design, the measured quantity should be insensitive to as many environmental variables as possible. One such approach in watt balance theory is to design a $1/r$ (r is the coil radius) magnetic field at the weighing position by either a electromagnetic system[2] or a symmetrical permanent magnet[12]. It has been mathematically proven that Bl is conserved in a pure $1/r$ magnetic field, which is therefore insensitive to any effects caused by undesired horizontal coil displacements or radially geometric fluctuations of the coil due to thermal expansion[13]. However, the generation of an ideal $1/r$ magnetic field strongly depends on concentrically aligning the inner and outer yoke, i.e., achieving horizontal r symmetry, proven to be a formidable challenge in practice. Our curiosity is whether Bl is still conserved when the r symmetry of the magnetic field is broken. To answer this question, we first give an analytical analysis of the asymmetrical magnetic field on a two dimensional field plane when the inner yoke and outer yoke are not concentric. The Bl is proven to remain a constant as in the symmetrical example. Without losing generality, the Bl conservation can be further extended by Gauss's law of magnetism on any two dimensional field planes by employing the magnetic monopole model[14]. This conclusion can be also explained by conformal transformations. The Bl conservation concept relaxes the design and alignment specifications required for a watt balance magnet.

The outline of the rest of this article is organized as follows: In section II, a typical watt balance magnet and the ideal symmetrical $1/r$ case is reviewed. In section III, an analysis of the asymmetrical case when the inner yoke and outer yoke are not concentric is presented, and the Bl conservation is shown. A more generalized extension of Bl conservation by employing the Gauss's law of magnetism and the conformal transformation is shown in section IV.

II. REVIEW OF AN IDEAL CASE WITH $1/r$ MAGNETIC FIELD

The analysis in this article is based on one of the most popular watt balance magnets employed[4,5,15,16]. Figure 1 shows the construction of the magnet with a symmetrical structure in both the r and z axes. The magnetic flux, generated by two permanent magnet disks oriented in repulsion, is guided by yokes of high permeability material through an air gap radi-

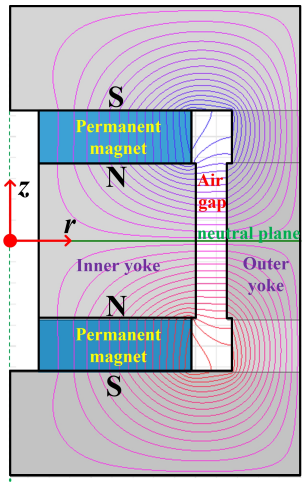

FIG. 1. A typical construction of the watt balance magnet (half cross sectional view). N and S denote the north and south poles of the permanent magnet. The magnetic flux lines through the circuit are shown. A similar watt balance magnet is employed in many NMI watt balances, e.g., the BIPM watt balance[5], METAS-II watt balance[4], NIST-4 watt balance[15], KRISS watt balance[16].

ally separating the inner and outer yokes.

Based on magnetostatic equations, $\nabla\cdot\mathbf{B}=\mathbf{0}$ and $\nabla\times\mathbf{B}=\mathbf{0}$, the magnetic field in the air gap can be described in the cylindrical coordinate as[17]

$$\frac{1}{r}\frac{\partial[rB_r(r,\phi,z)]}{\partial r}+\frac{1}{r}\frac{\partial B_\phi(r,\phi,z)}{\partial\phi}+\frac{\partial B_z(r,\phi,z)}{\partial z}=0, \quad (4)$$

$$\frac{1}{r}\frac{\partial B_z(r,\phi,z)}{\partial\phi}-\frac{\partial B_\phi(r,\phi,z)}{\partial z}=0, \quad (5)$$

$$\frac{\partial B_r(r,\phi,z)}{\partial z}-\frac{\partial B_z(r,\phi,z)}{\partial r}=0, \quad (6)$$

$$\frac{1}{r}\frac{\partial[rB_\phi(r,\phi,z)]}{\partial r}-\frac{1}{r}\frac{\partial B_r(r,\phi,z)}{\partial\phi}=0. \quad (7)$$

For the ideal case, the magnet shown in figure 1 is symmetrically constructed in both r and z directions, thus we have $B_\phi=0$, $\partial B_r(r,\phi,z)/\partial\phi=0$ and $\partial B_z(r,\phi,z)/\partial\phi=0$. Then equations (4)-(7) turns to

$$\frac{1}{r}\frac{\partial[rB_r(r,z)]}{\partial r}+\frac{\partial B_z(r,z)}{\partial z}=0, \quad (8)$$

$$\frac{\partial B_r(r,z)}{\partial z}-\frac{\partial B_z(r,z)}{\partial r}=0. \quad (9)$$

Equations (8) and (9) show that the two magnetic flux density components, B_r and B_z, are coupled. In watt balance operations, the weighing is conducted at the neutral plane of

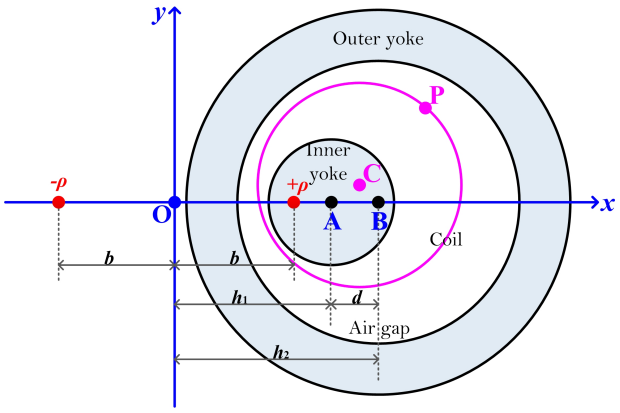

FIG. 2. The magnet and coil dimensions on the $z=0$ plane. A and B are centers of the inner yoke and outer yoke respectively while C is the coil center.

the magnet, i.e. $z=0$. Since the vertical magnetic field component is zero on the $z=0$ plane, the magnetic flux density contains a pure B_r component and is solved as

$$B_r(r,0)=\frac{r_cB_r(r_c,0)}{r}=\frac{\mathscr{B}}{r}, \quad (10)$$

where r_c is the coil radius and $\mathscr{B}$ is the product of $B_r(r,0)$ and r. It has been mathematically proven in[13] that the Bl at the neutral plane is independent from the coil horizontal position and the coil radius, i.e.,

$$(Bl)_{z=0}=2\pi r_cB_r(r_c,0)=2\pi\mathscr{B}. \quad (11)$$

III. Bl CONSERVATION IN ASYMMETRICAL MAGNETIC FIELD

A. Analytical expression of the magnetic field

Here we give an analytical solution of the magnetic field when the inner and outer yokes are not concentrically aligned. The magnet and coil geometric relationships on the $z=0$ plane have been shown in figure 2. Two boundary lines, the outer radius of the inner yoke (IY) and the inner radius of the outer yoke (OY), are considered equipotential, whose magnetomotive forces (MMFs) are set F and 0. The radii of IY and OY are r_1 and r_2 respectively, and their centers are separated by a distance d. The coil (radius r_c) is located in the air gap between IY and OY.

The model of magnetic monopoles was introduced in 1931 by Dirac in his famous work, i.e., Dirac quantization condition[18]. It assumes the existence of a magnetic field density, yielding magnetic charges measured in SI unit A·m. By introducing the magnetic charges, Maxwell's equations become beautifully symmetrical and a magnetic boundary problem can be equivalent to a conductive boundary problem in electrostatics[19]. Therefore, the method of image can be employed here to solve the magnetic field in the air gap region.

Without losing generality, the x axis is set along the maximum/minimum air gap, and the y axis coincides with the electrical axis. Two point monopole charges, $+\rho$ and $-\rho$, are placed in mirror at $(b, 0)$ and $(-b, 0)$ where b is an unknown variable. The distance of OA and OB, h_1 and h_2, are also unknown quantities. Based on the image method, we obtain[20]

$$r_1^2 + b^2 = h_1^2, \quad r_2^2 + b^2 = h_2^2, \quad h_2 - h_1 = d. \tag{12}$$

The unknown b can be solved in equation (12), i.e.,

$$b = \sqrt{\left(\frac{r_2^2 - r_1^2 - d^2}{2d}\right)^2 - r_1^2}. \tag{13}$$

Ignoring all boundaries in figure 2 and replacing the whole region with air, the magnetic potential φ on the xy plane can be calculated as

$$\varphi(x, y) = \frac{\rho}{4\pi\mu_0} \ln \frac{(x+b)^2 + y^2}{(x-b)^2 + y^2}, \tag{14}$$

where μ_0 is the permeability of the vacuum (air). The magnetic field $H = B/\mu_0$ is the partial derivative of the magnetic potential φ, which can be calculated as

$$B_x = \mu_0 \frac{\partial \varphi}{\partial x} = \frac{\rho b(y^2 - x^2 + b^2)}{\pi[(x-b)^2 + y^2][(x+b)^2 + y^2]}, \tag{15}$$

$$B_y = \mu_0 \frac{\partial \varphi}{\partial y} = -\frac{2\rho b x y}{\pi[(x-b)^2 + y^2][(x+b)^2 + y^2]}. \tag{16}$$

B. Numerical simulation of Bl

As is known, the geometrical factor Bl is defined as

$$Bl = \int_L (\mathbf{B} \times \mathrm{dl}) \cdot \mathbf{k}, \tag{17}$$

where L is the integral path along the coil, and $\mathbf{k}$ is a unit vector. In our analysis, the coordinate of the coil center, i.e., point C shown in figure 2, is set (x_0, y_0). For an arbitrary point P on the coil, its coordinate can be expressed as $(x_0 + r_c\cos\theta, y_0 + r_c\sin\theta)$ where θ is the angle of PCx. According to equations (15) and (16), two magnetic components at point P are calculated as

$$B_x(P) = \frac{\rho b[(y_0 + r_c\sin\theta)^2 - (x_0 + r_c\cos\theta)^2 + b^2]}{\pi\{[(x_0 + r_c\cos\theta) - b]^2 + (y_0 + r_c\sin\theta)^2\}} \times \frac{1}{[(x_0 + r_c\cos\theta) + b]^2 + (y_0 + r_c\sin\theta)^2}, \tag{18}$$

$$B_y(P) = -\frac{2\rho b(x_0 + r_c\cos\theta)(y_0 + r_c\sin\theta)}{\pi\{[(x_0 + r_c\cos\theta) - b]^2 + (y_0 + r_c\sin\theta)^2\}} \times \frac{1}{[(x_0 + r_c\cos\theta) + b]^2 + (y_0 + r_c\sin\theta)^2}. \tag{19}$$

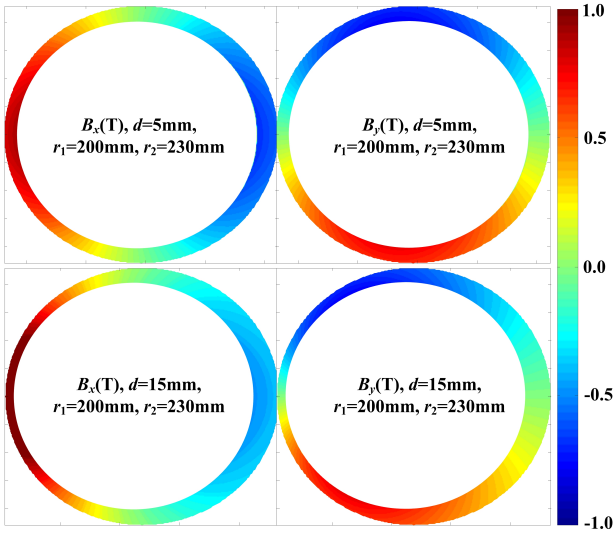

FIG. 3. The magnetic flux density distribution of B_x and B_y in the air gap when $d = 5$ mm and $d = 15$ mm. In the calculation, r_1 and r_2 are set as 200 mm and 230 mm.

Since the vector $\mathrm{dl}(P) = r_c(-\sin\theta, \cos\theta)\mathrm{d}\theta$, Bl can be rewritten as

$$Bl = \int_0^{2\pi} r_c[B_x(P)\cos\theta + B_y(P)\sin\theta]\mathrm{d}\theta. \tag{20}$$

To be sample, numerical simulation of the magnetic field distribution and Bl calculation is demonstrated in several examples. Figure 3 shows the numerical simulation of the magnetic flux density distribution of B_x and B_y in the air gap when $d = 5$ mm and $d = 15$ mm. It is apparent that the magnetic field strength is inversely proportional to the air gap distance.

We select five cases with different parameters to show how the integral function, i.e., $\Delta = r_c[B_x\cos\theta + B_y\sin\theta]$, varies as a function of θ. The parameters and Bl calculation results are listed in table I, and $\Delta(\theta)$ are shown in figure 4. It is shown that compared to the ideal $1/r$ field case (Δ is a constant), the variation of Δ at different θ locations is completely neutralized, and the Bl is shown in these examples to be constant and independent from a symmetrically changing the coil radius r_c, the IY and OY misalignment d and the coil position (x_0, y_0). Note that in the Bl calculation, we use 500 steps for the numerical integration, and it is found that the result unvaried when smaller or larger integration steps are employed.

IV. EXTENSION AND EXPLANATION OF THE Bl CONSERVATION

A. Gauss's law on magnetism

As a matter of fact, the Bl conservation can be extended to any two dimensional magnetic field planes. Here we give a brief proof using the Gauss's law for magnetism with a

TABLE I. Parameters setup and calculation result of the simulation examples.

Case No.	r_c (mm)	d (mm)	$x_0 - h_1 - d$ (mm)	y_0 (mm)	Bl (Tm)
1	215	5	-5	-5	1.00000000
2	220	5	-5	-5	1.00000000
3	215	15	-5	-5	1.00000000
4	215	5	5	-5	1.00000000
5	215	5	-5	5	1.00000000

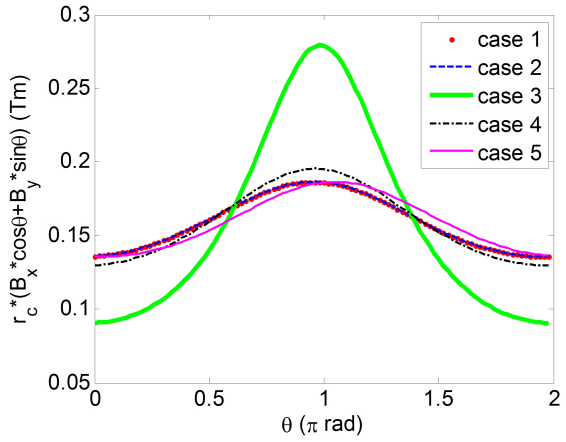

FIG. 4. The calculation result of the integral function Δ as a function of θ in different parameter setups. The case number is the same as the number shown in table I.

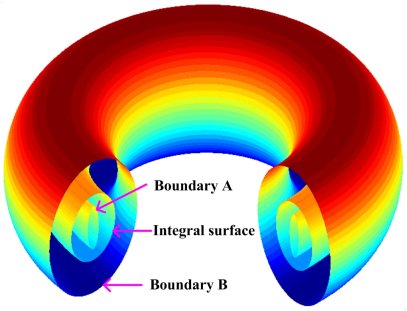

FIG. 5. The three dimensional space obtained by rotating the two dimensional field plane (3/4 view).

model of magnetic monopoles. Revising Gauss's law for magnetism[19], we have

$$\oint_S \mathbf{B} \cdot d\mathbf{A} = \frac{\rho_m}{\mu_0}, \tag{21}$$

where S denotes a closed surface, $d\mathbf{A}$ a vector whose magnitude is the area of an infinitesimal piece of the surface S, pointing outward, ρ_m the theoretical magnetic charge and μ_0 the permeability of free space.

It has been noticed that the Bl is calculated in terms of a cross product in equation (17) rather than a dot product in equation (21). In order to apply the Gauss's law of magnetism, we firstly show how the Bl is related to the magnetic flux in

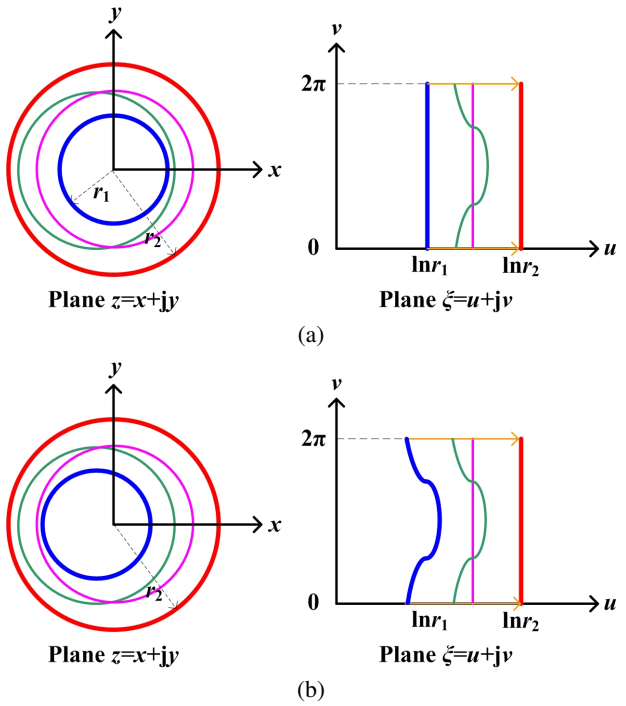

FIG. 6. The conformal transformations of different alignment cases for concentrically aligning the IY and OY. (a) shows an ideal symmetrical case with different coil positions and (b) presents the misalignment case with a same setup of coil position. The blue line and red line denote IY and OY respectively. The pink line is the ideal coil position while the green line is an arbitrary coil position. On the xy plane, the origin of coordinate is placed at the OY.

two dimensional vectors. $\mathbf{B} \times d\mathbf{l}$ can be expanded

$$\begin{aligned} \mathbf{B} \times d\mathbf{l} &= (B_x, B_y) \times (-r_c \sin\theta, r_c \cos\theta) \\ &= B_x r_c \cos\theta + B_y r_c \sin\theta, \end{aligned} \tag{22}$$

while the dot product of the vector $\mathbf{B}$ and the vector $d\mathbf{n} = (r_c \cos\theta, r_c \sin\theta)$ ($d\mathbf{n}$ is the normal of $d\mathbf{l}$) is calculated as

$$\begin{aligned} \mathbf{B} \cdot d\mathbf{n} &= (B_x, B_y) \cdot (r_c \cos\theta, r_c \sin\theta) \\ &= B_x r_c \cos\theta + B_y r_c \sin\theta. \end{aligned} \tag{23}$$

A comparison of equations (22) and (23) yields $\mathbf{B} \times d\mathbf{l} = \mathbf{B} \cdot d\mathbf{n}$, which shows in a two dimensional field plane Bl can be calculated by integrating the magnetic flux along the coil.

Secondly, we rotate the two dimensional magnetic field plane along a uniform circle, yielding a three dimensional space shown in figure 5. In the watt balance case, boundaries A and B are formed by rotating lines IY and OY while the integral surface is created by the coil. Figure 5 is a typical expression of Gauss's law. Assuming the total magnetic charge on the boundary A is ρ_m, the geometrical factor Bl is determined as

$$Bl = \frac{\rho_m}{2\pi\mu_0}. \tag{24}$$

Equation (24) shows the Bl of a watt balance coil is only determined by the magnetic charge ρ_m, independent of the

yoke shape, the alignment of the inner and outer yokes, the coil position and the coil shape.

B. Conformal transformation

The conformal transformation, or the conformal mapping, has an excellent property to modify only the geometry of a polygonal structure, preserving its physical magnitudes[21]. The Bl conservation in a two dimensional magnetic field plane can also be simply explained by conformal transformations. The following conformal transformation is applied, i.e.,

$$\xi = \ln z, \tag{25}$$

where $z = x + \mathrm{j}y$ denotes the xy plane, and $\xi = u + \mathrm{j}v$ is the transformation plane. Figure 6 presents the conformal transformations of the ideal symmetrical and the asymmetrical cases for concentrically aligning the IY and OY. Note that there is no fringe effect in the conformal transformation of equation (25). It can be seen that the transformation on the ξ plane is comparable to a capacitor with parallel or non parallel plates. Since the Bl is proportional to flux through the coil in the normal direction, for a two plate capacitor, the flux through the coil (the line between two plate lines) should be a constant only related to the charge of the high potential plate. Therefore, Bl is independent to the yoke misalignments in r direction and the coil horizontal displacements.

V. CONCLUSION

For watt balances, the Bl is independent from horizontal coil displacements in a $1/r$ magnetic field but the $1/r$ symmetry of the magnetic field strongly depends on the alignment of the IY and OY. We presented an analytical calculation of the magnetic field distribution when the r symmetry of the magnet is broken, i.e., IY and OY are not concentrically aligned. The analysis shows that Bl conservation is independent of the r symmetry of the magnetic field in the neutral plane $z = 0$. The Bl conservation established on any arbitrary, pure two dimensional magnetic plane, is proven by Gauss's law of magnetism or conformal transformations. This generalized Bl conservation analysis can provide insight for a much more relaxed construction and alignment procedure for watt balance magnets.

* Department of Electrical Engineering, Tsinghua University, Beijing 100084, China; leeshisong@sina.com

[1] Robinson I A 2012 Towards the redefinition of the kilogram: a measurement of the Planck constant using the NPL Mark II watt balance *Metrologia* **49** 113-56

[2] Schlamminger S, Haddad D, Seifert F, et al 2014 Determination of the Planck constant using a watt balance with a superconducting magnet system at the National Institute of Standards and Technology *Metrologia* **51** S15-S24

[3] Sanchez C A, Wood B M, Green R G, et al 2014 A determination of Planck's constant using the NRC watt balance *Metrologia* **51** S5-S14

[4] Baumann H, Eichenberger A, Cosandier F, et al 2013 Design of the new METAS watt balance experiment Mark II *Metrologia* **50** 235-42

[5] Fang H, A Kiss, E de Mirand, et al 2013 Status of the BIPM watt balance *IEEE Transactions on Instrumentation and Measurement* **62** 1491-98

[6] Thomas M, Espel P, Ziane D, et al 2015 First determination of the Planck constant using the LNE watt balance *Metrologia* **52** 433-44

[7] Kibble B P 1976 A measurement of the gyromagnetic ratio of the proton by the strong field method *Atomic Masses and Fundamental Constants 5* 545-51

[8] Mills I M, Mohr P J, Quinn T J, et al 2006 Redefinition of the kilogram, ampere, kelvin and mole: a proposed approach to implementing CIPM recommendation 1 (CI-2005) *Metrologia* **43** 227-46

[9] Hamilton C A 2000 Josephson voltage standards *Review of scientific instruments* **71** 3611-23

[10] Jeckelmann B, Jeanneret B 2001 The quantum Hall effect as an electrical resistance standard *Reports on Progress in Physics* **64** 1603-55

[11] Taylor B N, Witt T J 1989 New international electrical reference standards based on the Josephson and quantum Hall effects *Metrologia* **26** 47-62

[12] Li S, Schlamminger S, Pratt J 2014 A nonlinearity in permanent-magnet systems used in watt balances *Metrologia* **51** 394-401

[13] Li S, Schlamminger S, Haddad D, et al 2015 Coil motion effects in watt balances: a theoretical check, submitted to *Metrologia*.

[14] Bch A, Van Boxem R, Van Tendeloo G, et al 2014 Magnetic monopole field exposed by electrons *Nature Physics* **10** 26-9

[15] Seifert F, Panna A, Li S, et al 2014 Construction, measurement, shimming, and performance of the NIST-4 magnet system *IEEE Transactions on Instrumentation and Measurement* **63** 3027-38

[16] Kim D, Woo B C, Lee K C, et al 2014 Design of the KRISS watt balance *Metrologia* **51** S96-S100

[17] Li S, Yuan J, Zhao W, et al 2015 Field representation of a watt balance magnet by partial profile measurements *Metrologia* **52** 445-53

[18] Dirac P A M 1931 Quantised singularities in the electromagnetic field *Proceedings of the Royal Society of London A: Mathematical, Physical and Engineering Sciences* **133** 60-72

[19] dos Santos R P 2015 Magnetic monopoles and dyons revisited: a useful contribution to the study of classical mechanics *European Journal of Physics* **36** 035022

[20] Ida N 2000 *Engineering electromagnetics* New York: Springer.

[21] Calixto W P, Alvarenga B, da Mota J C, et al 2010 Electromagnetic problems solving by conformal mapping: A mathematical operator for optimization *Mathematical Problems in Engineering* **2010** 742039